



Automated Height and Banking Control of Hydrofoil Ski

GENG5512 Final Report

Alishan Aziz

*School of Electrical, Electronic and Computer Engineering
The University of Western Australia*

Prof. Dr. Thomas Bräunl

*Renewable Energy Vehicle Project
The University of Western Australia*

(Word count: 7,416)

Abstract

Riding jet skis has become one of the most popular means of recreation particularly in coastal cities like Perth. Most people are out on lakes, rivers, or even the ocean, riding skis especially over the weekends. However, like most crafts, these skis consume fossil fuels and subsequently waste most of their energy crashing against waves. Even in skis that are electric, most of the added mass in batteries exists solely to compensate the energy lost crashing against waves.

A new class of electric hydrofoil skis are now in development across the world that overcome both these issues when ‘foiling’ – the state in which the craft is lifted above water surface. Additional advantages of hydrofoil skis include longer riding range and time, effective energy consumption, and fewer batteries required in-craft compared to traditional electric skis. The University of Western Australia’s (UWA) Renewable Energy Vehicle (REV) Project has a hydrofoil ski in development.

The skillsets required to ride a hydrofoil are different from those required for a traditional ski. In crude sense, required skills can be considered an amalgamation of motorcycle skills and traditional ski skills. To make hydrofoil skis more accessible to the public, embedded control systems must take over the complex tasks of height control and banking based on sensor feedback of height, pitch, roll, and yaw. This project involved developing control algorithms implemented in the central microcontroller to effectively address these control requirements.

PID control implementation is worked on for controlling servo motors adjusting the hydrofoil aileron angle of attack (producing lift and banking) as well as adjusting pulse-width modulation (PWM) that controlled speed of motors to achieve differential speeds for turning when craft is not foiling. Revisions to algorithms implemented are done based on experimental tests performed on the prototype in water.

Complementary work done in successful pursuit of this project include designing of Controller-Area Network (CAN) architecture and Graphical User Interface (GUI) to display and log relevant information of hydrofoil performance.

Acknowledgements

I express my deepest gratitude to Prof. Thomas Bräunl for his guidance, support, direction, and knowledge in the pursuit of this project.

I also thank Eric Metrot, one of the project owners, and all the ski project students I have worked with namely Layla Krishna, Liyang Xu, Jeremy Guo, Ben Ness, Vladimir Pavkov, and the students from the REV autonomous bus team – Farhad Ahmed and David Gregory for their time and diligence in getting the craft functional.

I extend my appreciation and gratitude to Pierre-Louis Constant for imparting his experience, time, knowledge, and resources to me throughout the course of this project.

I remain indebted to my mentor, Marcus Pham, who encourages me to be passionate about all things I build, and from whom I continue to absorb proficiency in engineering.

I thank all my friends who keep encouraging me to perform to the best of my abilities.

Lastly, I thank my mother and sister who give me strength to keep going each day. They are the motivation and drive behind all I do.

TABLE OF CONTENTS

ABSTRACT	I
ACKNOWLEDGEMENTS	II
NOMENCLATURE	VI
1. INTRODUCTION	1
2. PROBLEM STATEMENT	3
3. CONTRIBUTIONS	4
4. LITERATURE REVIEW	4
4.1 HYDROFOIL	4
4.1.1 <i>What is a hydrofoil?</i>	4
4.1.2 <i>Function of Ailerons</i>	5
4.1.3 <i>Closed loop control</i>	6
4.1.4 <i>Hydrofoil height control</i>	7
4.1.5 <i>Hydrofoil banking</i>	7
4.1.6 <i>Differential drive</i>	8
4.2 CONTROLLER AREA NETWORK COMMUNICATION	8
4.3 BATTERY MANAGEMENT SYSTEM (BMS).....	9
4.4 QT AND QML	11
5. TOOLS USED	11
5.1 MAIN HARDWARE	11
5.1.1 <i>APM2.7 (ArduPilot MEGA 2.7)</i>	11
5.1.2 <i>Battery and BMS</i>	12
5.1.3 <i>VESC-6</i>	13
5.1.4 <i>Grayhill 3D70 Display</i>	14
5.2 SOFTWARE USED.....	15
5.2.1 <i>VESC Tool</i>	15
5.2.2 <i>Qt Creator</i>	16
6. METHODOLOGY	17
6.1 CONTROL OVERVIEW	17
6.2 HEIGHT CONTROL.....	18
6.3 BANKING CONTROL	19
6.3.1 <i>Motor differential drive</i>	20
6.3.2 <i>Foiling turn (pure aileron control)</i>	20
6.4 VESC INTEGRATION.....	21
6.5 GUI DESIGN.....	22
7. RESULTS AND DISCUSSIONS	23
7.1 HEIGHT CONTROL.....	23
7.2 BANKING CONTROL	24
7.3 CAN INTEGRATION, & GUI.....	25
7.4 WIRING & CONTROL BOX ORGANISATION	27
7.5 PERFORMANCE	27
8. CONCLUSION AND FUTURE SCOPE	28
8.1 CONTROLLER	28
8.2 HARDWARE MODULES & TELEMETRY	28
8.3 PRINTED CIRCUIT BOARD (PCB) DESIGN.....	29
9. REFERENCES	30

APPENDIX A: EXTENDED CAN FRAME	34
APPENDIX B: BMS CAN PROTOCOL	34
APPENDIX C: VESC6 CAN PROTOCOL.....	35
APPENDIX D: VESC TOOL ESC CAN CONFIGURATION.....	36

LIST OF FIGURES

Figure 1: EV uptake by country over the last decade graph taken from [2]	1
Figure 2: REVski crashing into waves copied from [4].....	2
Figure 3: REV Hydrofoil WaveFlyer copied from [5]	2
Figure 4: Nomenclature of general hydrofoil as taken from [9].....	4
Figure 5: Resultant loads on hydrofoil copied from [9]	5
Figure 6: Aileron pitch control effect profile view.....	5
Figure 7: Aileron movement direction for roll (banking) control.....	6
Figure 8: Comparison of motor step-response for PD & PID controllers, taken from [15]	6
Figure 9: Banking angles at different aircraft velocities, copied from [19].....	8
Figure 10: Differential Drive on the hydrofoil ski.....	8
Figure 11: Reduction in wiring and complexity using CAN. Image copied from [24].....	9
Figure 12: CAN versions. Table taken from [24]	9
Figure 13: Extended CAN Frame format taken from [23]	9
Figure 14: Parts of a Battery	10
Figure 15: Qt Overview diagram obtained from [27].....	11
Figure 16: ArduPilot Mega	11
Figure 17: APM2.7 used in the hydrofoil ski.	12
Figure 18: Samsung INR 18650 cells used in the hydrofoil ski [32]	12
Figure 19: ZEVA BMS16v2 [33]	13
Figure 20: VESC-6 mkIV with connectors and switches [37]	13
Figure 21: Flipsky ESC breakout diagram copied from [38]	14
Figure 22: Grayhill 3D70 display sample image copied from [39].	14
Figure 23: VESC Tool	15
Figure 24: Qt Creator Project Window	16
Figure 25: Qt Creator UI Designer	16
Figure 26: Overall control UML.....	17
Figure 27: Control Loop Simplified Diagram	18
Figure 28: Height control UML.....	19
Figure 29: Banking control overview	19
Figure 30: Motor movement direction during surface turn	20
Figure 31: Aileron movement direction when banking	20
Figure 32: Turning UML when ski is foiling.....	21
Figure 33: Display application UML.....	22
Figure 34: Stable height 'foiling'	23
Figure 35: 15° banking of hydrofoil ski.....	24
Figure 36: Hydrofoil Ski CAN Bus Schematic.....	25
Figure 37: Final implemented GUI on Grayhill 3D70.....	25
Figure 38: Control Box Wiring Schematic	26
Figure 39: Test riding route	27
Figure 40: Speed plot for a test run.....	27

Figure 41: BeagleBone Blue, copied from [43].....	28
Figure 42: Samsung waterproof tablet with GPS, Bluetooth Figure 42	29
Figure 43: CAN settings on VESC Tool	36

LIST OF TABLES

Table 6-1: Motor parameters	21
Table 0-1: BMS Status Transmitted Packet obtained from [35].....	34
Table 0-2: Cell Voltage packets from BMS16 copied from [34]	34
Table 0-1: CAN status packets transmitted by VESC-6.....	35

Nomenclature

ACK	Acknowledgement
ADC	Analog to Digital Converter
APM	ArduPilot MEGA
BMS	Battery Management System
CAN	Controller Area Network
CRC	Cyclic Redundancy Code
DC	Direct Current
DLC	Data Length Code
DMP	Digital Motion Processor
EOF	End of Frame
ePWC	Electric Personal Watercraft
ERPM	Electrical Revolutions per Minute
ESC	Electronic Speed Controller
EV	Electric Vehicle
GPS	Global Positioning System
GUI	Graphical User Interface
I2C	Inter-Integrated Circuit
IDE	Integrated Development Environment
IDE ₂	Identifier Extension
IFS	Interframe Space
IMU	Inertial Measurement Unit
Kbps	Kilobit(s) per second
LED	Light Emitting Diode
Mbps	Megabit(s) per second
PID	Proportional Integral Differential
PPM	Pulse-Position Modulation
P2P	Point-to-Point
PWC	Personal Watercraft
PWM	Pulse-Width Modulation
QML	Qt Meta-Object Language
REV	Renewable Energy Vehicle Project
RPM	Revolutions per Minute
SoC	State of Charge
SOF	Start of Frame
SRR	Substitute Remote Request
STM	STMicroelectronics
SWD	Serial Wire Debug
UART	Universal Asynchronous Receiver Transmitter
UI	User Interface
UML	Unified Modelling Language
USA	United States of America
USB	Universal Serial Bus
UWA	The University of Western Australia
VESC	Vedders Electronic Speed Controller
ZEVA	Zero Emission Vehicles Australia

1. Introduction

The personal watercraft (PWC) was initially created as a single-seater machine for recreational and commutation projects on water but has evolved since into two- and three-person crafts popular today with families and enthusiasts alike. In 2004 the National Marine Manufacturers Association, USA, reported that approximately 20 million Americans ride PWCs each year [1].

PWCs today have become an integral part of family recreation. Almost all PWCs sold are fuel-injected with four-stroke engines. Consequently, they are a source of air, water, and noise pollution. Foremost water quality concern is discharge of unburnt fuel into the water. Air pollution stems from discharge of burnt fumes into the atmosphere while the PWC is operational. Noise pollution is caused by two sources [1]:

1. Operation of engines.
2. Water splashing and crashing against PWC hull.

Removing combustion engines helps curb water, air, and noise pollution which is exactly what electrification of PWCs achieves.

Technological advancements in electrification of all kinds of automotive – cars, buses, trucks, etc– continue to progress at an unprecedented rate. Global electric car sales alone registered a 40% year-on-year increase in 2019 compared to 2018 [2]. This trend continued into 2020 despite a global shrink in overall car sales. The takeaway here is clear – the necessity and market for electric vehicles are expanding. EVs also have the benefit of lower maintenance, fewer moving parts, enhanced air pollution, smoother driving experience, and better energy security [3]. This further incentivises development of electric PWCs.

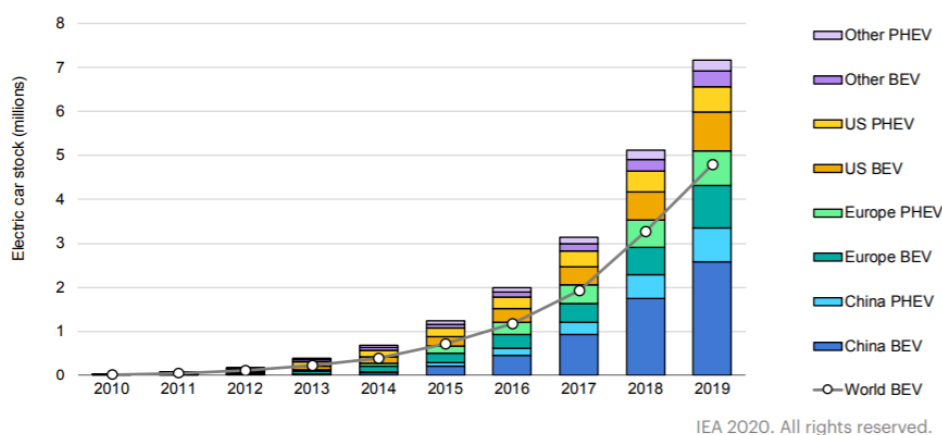


Figure 1: EV uptake by country over the last decade graph taken from [2]

The University of Western Australia’s (UWA) Renewable Energy Vehicle Project (REV) Team successfully converted a 2008 sea-doo to a fully electric PWC (e-PWC) named ‘REVSki’ which can provide 25 minutes range, support 2 passengers, and reach a top speed of 41kmph. It provides the performance of a traditional PWC minus the noise and pollution [4].

While the project was an astounding success, a good fraction of energy of the PWC remains wasted in crashing into and overcoming waves, limiting range to just 25 minutes out of 7.6kWh energy. Raising the PWC above water surface overcomes this expenditure of energy and is the principle behind hydrofoil PWCs.

The REV team developed the world's first electric hydrofoil PWC in 2019. Performance was "much quieter, more energy efficient, and produces no emissions". With just 2kWh of energy a range of 30 minutes was obtained [5].



Figure 2: REVski crashing into waves copied from [4]



Figure 3: REV Hydrofoil WaveFlyer copied from [5]

However, challenges, highlighted in section 2 blow, inhibit easy adoption and convenient riding of hydrofoil skis. Emphasis currently is on rider's ability to both elevate and bank the ski. This project aims to automate both processes.

Additionally, rider needs access to battery health information when riding the ski such as current draw, total pack voltage, amp hours remaining, and power being consumed. All this information is displayed in the form of huge numeric elements without provision to display motor or foiling information. This information should be presented in as simple and informative a way as possible to further ease adoption of hydrofoil skis. Knowing the amount of energy left will help rider identify the maximum height that can be achieved.

2. Problem statement

While the hydrofoil jet ski can lift the PWC with rider above water surface, controlling it requires experience and skill. Two aspects of riding the jet ski, height adjustment and banking, are left entirely to the rider.

Height control post lift-off is done manually by adjusting the angle of attack that ailerons make underwater. Joysticks on either side of the steering handle allow the rider to produce movements of ailerons with trim adjustment, enabling height control.

Banking is achieved by turning the steering handle and adjusting left trigger on the steering until a suitable turn is achieved. If an inexperienced rider attempts this manoeuvre, they are likely to get thrown off the ski from centrifugal force generated. Moreover, steering handle moves the entire mounting of rear hydrofoil. Precise control is impossible when the entire mounting swivels. Both motor controllers are controlled by the same PPM line as opposed to separate lines for differential control. Both these factors combined make the hydrofoil ski inconvenient to use.

If this project is to be a replacement for traditional jet skis, then both height and banking control should be handled by the internal embedded controller. Sensor inputs for pitch, roll, yaw, height above water, and desired steering angle are to be used to determine gain constants and control the angle made by ailerons with water without user intervention.

A CAN architecture must be implemented to integrate additional CAN-based devices within the ski. This will serve as a first step to transitioning to a complete CAN-based system. Advantages of using CAN in automotive that hold true even for watercrafts. The existence of such a network is currently restricted – it is limited to communication between BMS and the display.

The display configured with custom GUI for the hydrofoil ski fails to update elements such as current being drawn by motors, cell voltage, and speed, reliably in real-time. All data displayed are from the BMS. These elements occupy the entire screen real estate incomprehensively. GUI re-design is necessary to ensure more data can be effectively placed on the display.

3. Contributions

To address the issues laid out in section 2, the following work has been accomplished:

Height control algorithm implemented on the control unit, APM2.7, to try and keep the hydrofoil 30cm above water surface. Control is achieved based on height sensor feedback. Different sensors were tested by other members of the REV project, but the core algorithm implemented is sensor independent. As the craft gets closer to the desired height, angle of attack made by the ailerons is reduced.

The banking control algorithm implemented on the APM2.7 went through two main overhauls. In the final algorithm implemented, if craft is in 'flight mode', then both motors maintain the same speed and banking is achieved through the ailerons. Flowcharts and further details of control methodology are explained in section 6.

Hardware redesign and control box with CAN architecture is implemented to minimise noise in the system and ensure all signals are received and transmitted error-free. Motor controllers moved into the craft as opposed to outside the craft from previous design to reduce travel length for motor controller PWM signals. This effectively minimises noise.

A new GUI is also implemented on the craft's display to present all relevant information of power, current, voltage, duty cycle, and motor controller temperatures to the rider.

4. Literature Review

4.1 Hydrofoil

4.1.1 What is a hydrofoil?

The main function of a hydrofoil is to lift the hull of PWC outside water. At low speeds, the PWC hull sits in the water with hydrofoils completely submerged. As the craft's speed increases, high speed fluids around hydrofoils create lift. Beyond a threshold speed, this lift produced will be equal to the sum of craft and craft's cargo weights at which point PWC hull is lifted outside water surface enabling it to achieve higher speeds [6, 7, 8].

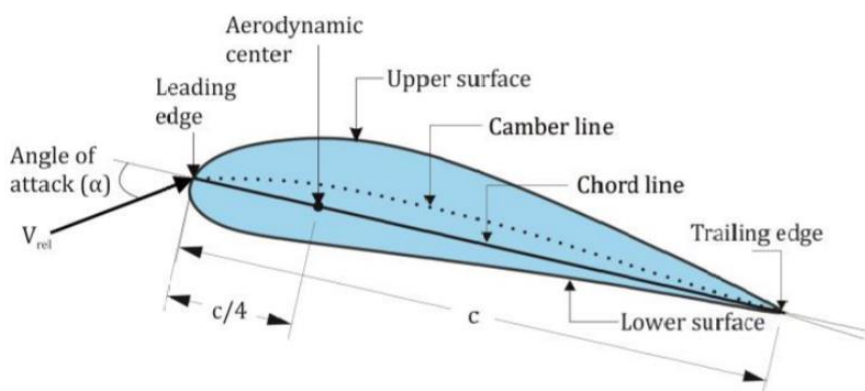


Figure 4: Nomenclature of general hydrofoil as taken from [9]

Shape and different parts of a general hydrofoil are indicated in Figure 4. Curvature of the upper surface of hydrofoils is more than that of the lower surface. When submerged in stream

flow, the hydrofoil is subject to various forces due to pressure and velocity changes and viscosity of the fluid. These forces are represented as drag force, F_D , lift force, F_L , and pitching moment M_P (Figure 5).

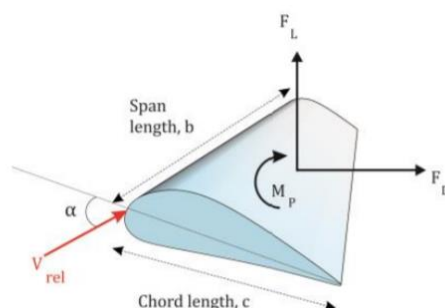


Figure 5: Resultant loads on hydrofoil copied from [9]

Higher velocity particles at the upper surface generate a low-pressure zone while low velocity particles at the lower surface generate a high-pressure zone. Hence, curvature of hydrofoils results in unequal pressures at the two surfaces, which, along with viscous forces, increases F_D . This unequal pressure between the surfaces also creates lift force. Direction of lift force is along the chord line shown in Figure 4 [9]. Since these forces are vectors, effect of resultant force lifts the PWC above water surface.

There are two main hydrofoil configurations commonly in use: submerged type and surface-piercing type, though several other types have been explored in the past [10]. The former has two key features [11]:

1. Superior sea-state capability, i.e., less subject to the effects of waves and hence more stable at sea.
2. Inherently roll unstable with no implicit attitude reference. In other words, they are not self-stabilising.

Hydrofoils used on the ski are the submerged type. The drawback of this system is that height control must be provided externally through controllers.

4.1.2 Function of Ailerons

Ailerons connected to the hydrofoil are important control surfaces especially when the craft is in 'flight mode' in much the same way they are for aircrafts. They are required to generate pitch control to adjust height, roll control to provide rolling motion for the ski to bank and turn, and yaw control for stability and turning when required.

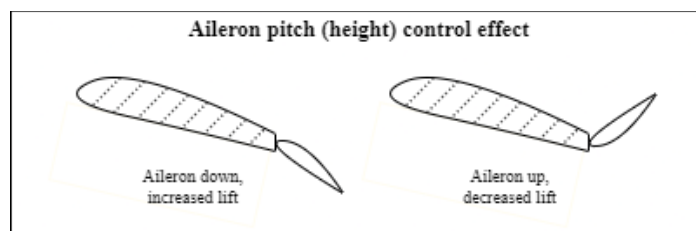


Figure 6: Aileron pitch control effect profile view.

Consider a single aileron to better understand its effects. If the aileron is lowered with respect to foil profile, fluid speed on the top of the foil increases, thereby increasing lift. If the same

aileron is lowered with respect to foil profile, fluid speed on the top of foil decreases, thereby decreasing lift. This phenomenon is indicated in Figure 6.

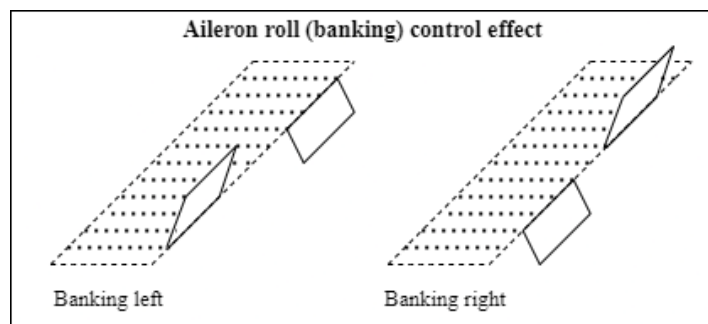


Figure 7: Aileron movement direction for roll (banking) control

For banking, ailerons need to be in opposite motion – if the right aileron is upwards, then the left will be downwards vice versa depending on direction of turn required. This creates an unbalanced sideways force on the craft causing a curve in flight path [12, 13]. When banking left, the left aileron is lowered decreasing its lift while the right aileron is raised increasing its lift. Consequently, the craft rolls towards the left and starts banking left. The opposite motion is used to bank right. These movements are depicted in Figure 7.

This phenomenon is leveraged in elevation, pitch, and roll control of aircrafts. In aircrafts as well as watercrafts, a rudder is normally used to achieve uniform yaw control. To the hydrofoil ski, however, no rudder is attached. Both height and banking control of ski are targeted using combinational control of both ailerons.

Lastly, with ailerons, there is a maximum angle of attack that provides maximum lift. If the angle of attack is raised beyond this angle of attack, lift decreases. A summary of effect of angle of attacks of hydrofoils is given in [14].

4.1.3 Closed loop control

A closed-loop control system is necessary especially for height control when depth sensor data is used to either lower or raise the jet ski. This section of the report briefly discusses the popular proportional-integral-differential (PID) closed-loop control [15].

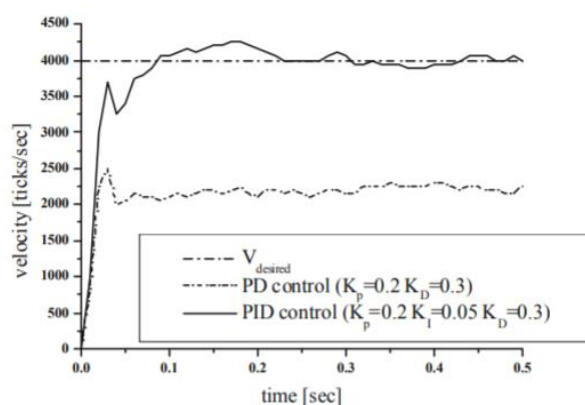


Figure 8: Comparison of motor step-response for PD & PID controllers, taken from [15]

In many applications, a sudden change in control value may not result in desired smooth behaviour. In such cases, a more advanced controller, the PID controller, is used. This

controller consists of three core parts – proportional, integral, and derivative. The integral term helps reduce steady-state error to zero. The derivative term speeds up the controller's response time with respect to a change in input [15]. A PID controller combines both these benefits—namely – reducing steady state error and speeding up controller's response time. Reaching equilibrium faster, shown in Figure 8: Comparison of motor step-response for PD & PID controllers, taken from .

4.1.4 Hydrofoil height control

If height of the ski above water is not regulated, two conditions arise [16]:

1. Hydrofoil gets lowered under water surface, resulting in hull of PWC encountering water. This increases hull resistance and ultimately culminates in a waste of energy in crashing against waves.
2. Hydrofoil moves closer to the water surface, resulting in a decrease in instantaneous lift force at the cost of flight stability.

Additionally, another challenge to hydrofoil control stems from balancing a large PWC on top of relatively small foils. For such systems, the controller can control states such as tracing reference height and pitch angle [8].

Some physical control mechanisms, such as improvements to physical foil structure, improvement of fore foil system, enhancing lift-drag ratio, etc., as detailed in [17], serve as a good baseline to understanding the importance of lift-drag ratio and how the angle of attack affects lift produce.

In [11], design for a special ultrasonic ranging device for measurement and control of submerged hydrofoil based PWC is discussed. Probes, being submerged, are susceptible to corrosion and impact with debris. Ultrasonic sensors are therefore found to be cost-effective and suitable for measuring height of ski above water surface.

PID controller mechanisms, detailed in section 4.1.3 and implemented in [18], are used to achieve height control.

4.1.5 Hydrofoil banking

Actuation of banking using aileron control is described in section 4.1.2. Banking depends on load and other geometric criteria, commencing from those indicated in [10].

In aircrafts, once banking has commenced, outer wing starts moving faster than inner wing, resulting in higher lift generated on the outer wing, triggering a downward spiral motion. For the hydrofoil craft, a 'gliding' turn is targeted in which water pressure on the aileron that is lower automatically compensates for the increase in lift due to velocity of the upper aileron, causing a smooth, gliding turn. These phenomena are explored in depth in [19].

The banking angle required for successful turning of the craft is dependent on speed of the craft. In the case of aircrafts, Figure 9 demonstrates this phenomenon. These angles are also dependent on radius of wing of the craft.

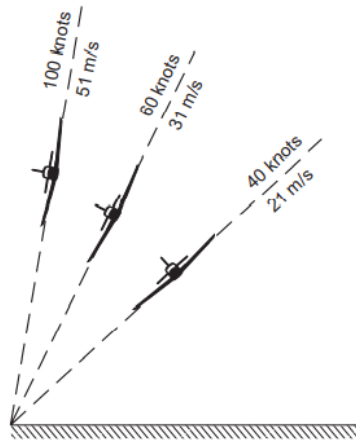


Figure 9: Banking angles at different aircraft velocities, copied from [19]

In case of the hydrofoil craft, a fixed banking angle is used irrespective of speed since

- Ski is much smaller than an aircraft.
- Speeds achieved by the hydrofoil craft are far inferior to those of an aircraft.

4.1.6 Differential drive

Differential drive system is composed of two motors fixed in positions on left and right side of the PWC, each individually controlled to move forward or turn [15, 20].

Differential drive is used in the ski since two different motor controllers, based on open-source Vedders Electronic Speed Controller (VESC) hardware, are used to control the speed of each of the motors individually. This arrangement based on that of a two-wheel motor drive vehicle [21], is shown in Figure 10. Each Pulse-Position Modulation (PPM) line actuates a separate motor. If the right motor moves faster than the left motor, craft turns left and vice-versa.

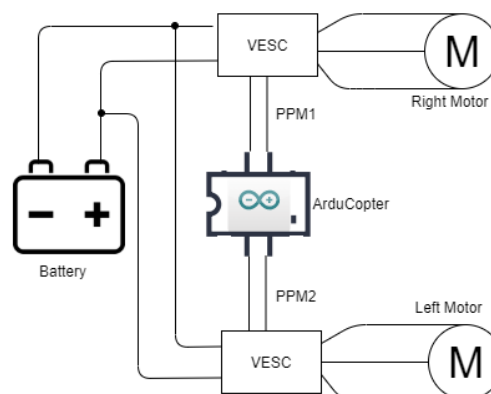


Figure 10: Differential Drive on the hydrofoil ski

4.2 Controller Area Network Communication

CAN is a multi-master communication protocol originally developed by Bosch for in-vehicle networks [22]. It supports up to a maximum signalling rate of 1 megabit per second (Mbps) [23]. Automotive manufacturers initially used point-to-point (P2P) wiring to connect all the electronics within the system. As the number of electronics kept increasing, this wiring became bulky and expensive to maintain. To overcome this issue, dedicated wiring was replaced with in-vehicle single-bus communication networks.

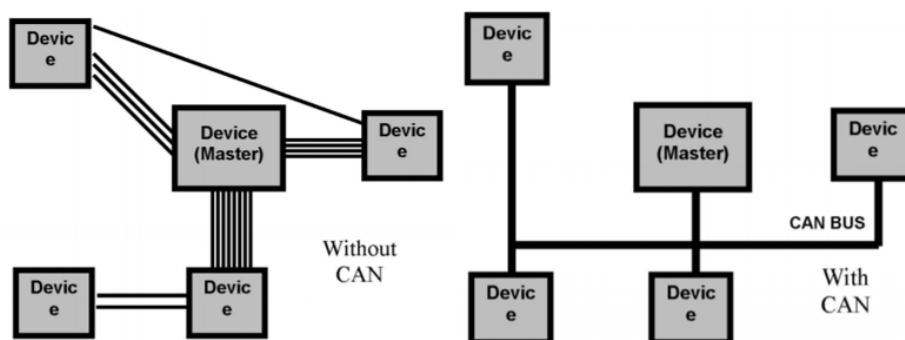


Figure 11: Reduction in wiring and complexity using CAN. Image copied from [24]

Generally, a twisted-pair cable is used to achieve high-integrity fast serial half-duplex communication speeds of up to 1Mbps between up to 40 devices. There are currently two standards dictating CAN physical layer operation based on speeds of communication achieved [24], shown in Figure 12.

	Standard	Signal Rate	Identifier
Low-Speed CAN	ISO 11519	125 kbps	11-bit
CAN 2.0 A	ISO 11898 (1993)	1 Mbps	11-bit
CAN 2.0 B	ISO 11898 (1995)	1 Mbps	29-bit

Figure 12: CAN versions. Table taken from [24]

Key benefits of using CAN [22, 23]:

1. Low-cost lightweight network: lesser wiring reduces costs and network weight.
2. Broadcast communication: All devices on the network are intelligent – they decide which of the bus messages are relevant to them.
3. Priority scheduling: Every device, or node, is assigned a priority.
4. Error capabilities: Cyclic Redundancy Code (CRC) is included in for error checking.
5. Fault confinement: Any faulty node in the CAN network is automatically dropped.

CAN frames are of two main types [23]: Standard (11-bit identifier) and Extended (29-bit identifier). These are differentiated purely by the identifier bits.

S O F	11-bit Identifier	S R R	I D E	18-bit Identifier	R T R	r1	r0	DLC	0...8 Bytes Data	CRC	ACK	E O F	I F S
-------------	-------------------	-------------	-------------	-------------------	-------------	----	----	-----	------------------	-----	-----	-------------	-------------

Figure 13: Extended CAN Frame format taken from [23]

Different bit fields in this frame are explained in Appendix A.

On the electric hydrofoil jet ski, extended CAN is used to share data between the BMS, motor controllers, and ski display.

4.3 Battery Management System (BMS)

Lithium cells, when fully charged, could reach dangerous high voltages rapidly. If one cell in a pack undergoes this rapid charge before other cells can be charged, then the total pack voltage

will be registered as fully charged even though some cells may be far from being fully charged [25]. Hence, voltage of each individual cell must be monitored instead of measuring voltage of the entire pack. This is done by the BMS.

Overall purpose of a BMS is [26]:

1. Provide battery longevity and safety.
2. Indicate the state-of-charge and health of cells.
3. Monitor temperature, current, voltage, and power of the cell pack and provide cautions whenever necessary.
4. Terminate load and notify user when cell capacity falls below set threshold.

Battery properties affecting capacity are stored energy, rated capacity, available capacity, and state-of-charge (SoC). Battery can be fundamentally split into three zones: inactive portion that is lost to aging of the cell, empty portion that can be recharged, and stored energy that can be used (Figure 14).

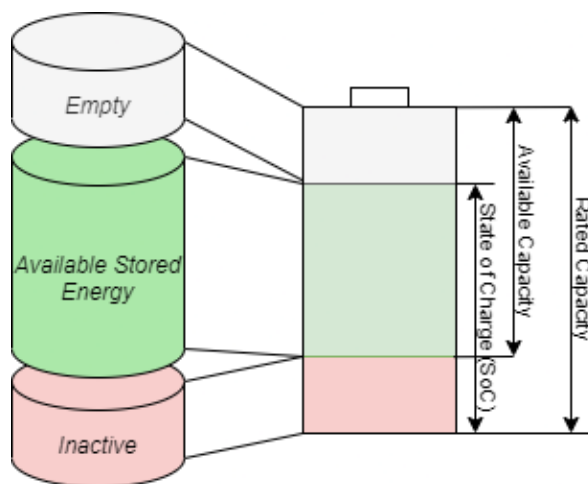


Figure 14: Parts of a Battery

A BMS measures the rate of charge flow and regulates current draw from cells. As soon as a cell voltage falls below a set threshold, load is turned off and no more current is drawn from cells. BMS used in the jet ski is the Zero Emission Vehicles Australia (ZEVA) BMS-16v2, discussed in section 5.1.2.

4.4 Qt and QML

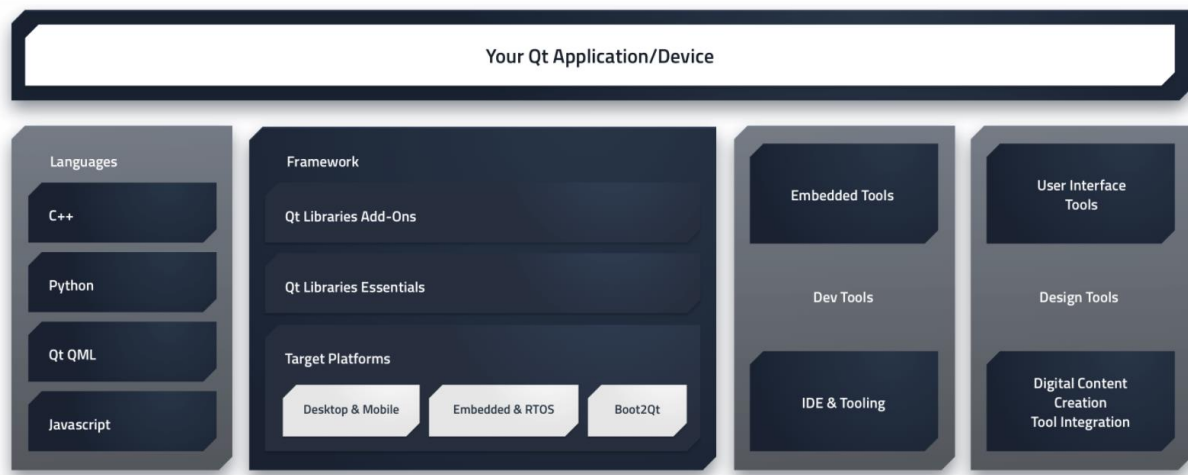


Figure 15: Qt Overview diagram obtained from [27]

Qt is a “cross-platform application development framework”, based on C++, suited for mobile, desktop, as well as embedded systems [28]. Qt is available as a free tool with its own built-in integrated development environment (IDE). The latest versions of Qt come bundled with a visual editor that allows seamless front-end UI design integration using an easy-to-use declarative language called Qt Meta-Object Language (QML) [29].

The ability to cross-compile code allows users to write code in, say, Windows, and deploy builds to embedded devices that are based on, say, Linux. This approach is taken when programming the display mounted on UWA REV’s Hydrofoil Ski.

5. Tools Used

5.1 Main Hardware

5.1.1 APM2.7 (ArduPilot MEGA 2.7)

APM is an Arduino Mega platform-based Inertial-Measurement-Unit (IMU) autopilot that can control fixed-wing aircrafts, multi-rotor helicopters, as well as traditional helicopters. It can handle autonomous stabilisation, waypoint-based navigation, and two-way telemetry [30].



Figure 16: ArduPilot Mega

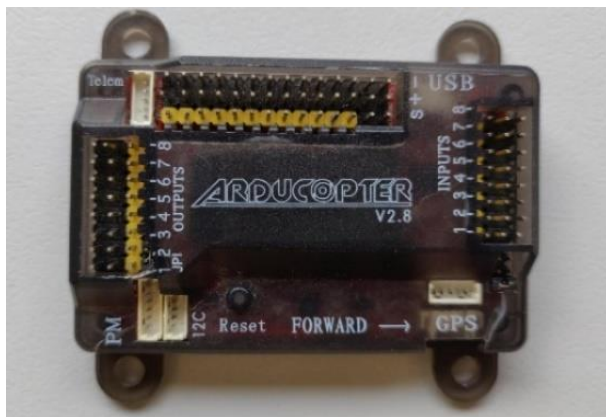


Figure 17: APM2.7 used in the hydrofoil ski.

APM is programmed using open-source tools such as Arduino IDE or the dedicated ArduPilot open-source control software. Key features of the ArduPilot Mega that make it an attractive choice include:

1. Free open-source firmware supporting multiple hardware devices.
2. Two-way telemetry and in-flight command.
3. 4MB of onboard data-logging memory.
4. Multiple servo output pins to control different servos and motors.
5. Analog as well as digital inputs.
6. I2C and USB ports.

5.1.2 Battery and BMS

Samsung SDI INR18650-30Q lithium-ion cells [31] are used in the REV hydrofoil ski in a 12-series 16-parallel (12S16P) configuration. Each cell has a nominal voltage of 3.6V and a cell capacity of 3000mAh, capable of discharging at 15A.



Figure 18: Samsung INR 18650 cells used in the hydrofoil ski [32]

A 16P configuration gives a total pack capacity of $3000 \times 16 = 48000\text{mAh} = 48\text{Ah}$.

Each cell can be charged to a maximum of 4.2V, giving a total installed pack voltage of $12 \times 4.2 = 50.4\text{V}$

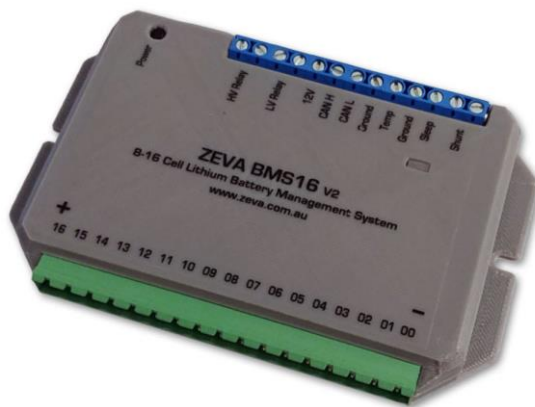


Figure 19: ZEVA BMS16v2 [33]

8-16 cell Lithium BMS from ZEVA with a 5-12000Ah capacity. This BMS can measure up to 500A current using built-in shunt interface and consumes up to 30mA current when running [34]. It also has temperature sensing, sleep mode, automatic pack balancing, and control interface through a monitor that make it responsive to changes in battery conditions as well as convenient to program and use.

BMS16v2 communicates over CAN bus at a baud rate of 250 Kilobits-per-second (Kbps) using CAN2.0B. BMS16 has four CAN screw-terminals for bus connections as per [35]. All relevant packet IDs transmitted by BMS16v2 are given in Appendix B. Batteries used in the hydrofoil ski have properties defined as per their datasheets in [32, 31].

5.1.3 VESC-6

The VESC-6 is an electronic speed controller capable of controlling 3-phase motors with adjustable current and voltage filters. It can detect any motor attached to it with precision and reliability, making it a suitable motor controller with the ability to plug-and-play with motors we already have [36].

Communication options with the VESC are plenty giving them an advantage over other ESCs. Configuration of any VESC-based motor controller is done using the VESC tool discussed in section 5.2.1. Two different VESC-6 based controllers were explored over the course of this project – Trampa VESC and Flipsky ESC.

5.1.3.1 Trampa VESC

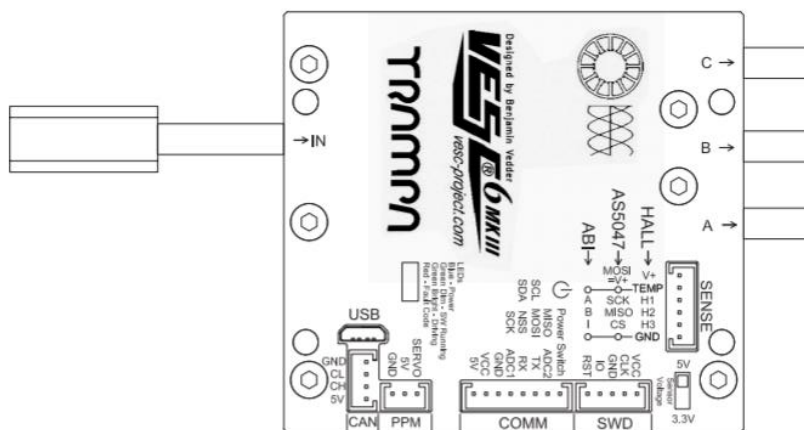


Figure 20: VESC-6 mkIV with connectors and switches [37]

This VESC (Figure 20) has the following ratings [36]:

1. Input Direct Current (DC) voltage between 6V-60V.
2. Continuous output current of 100A with bursts of 120A.

5.1.3.2 Flipsky VESC

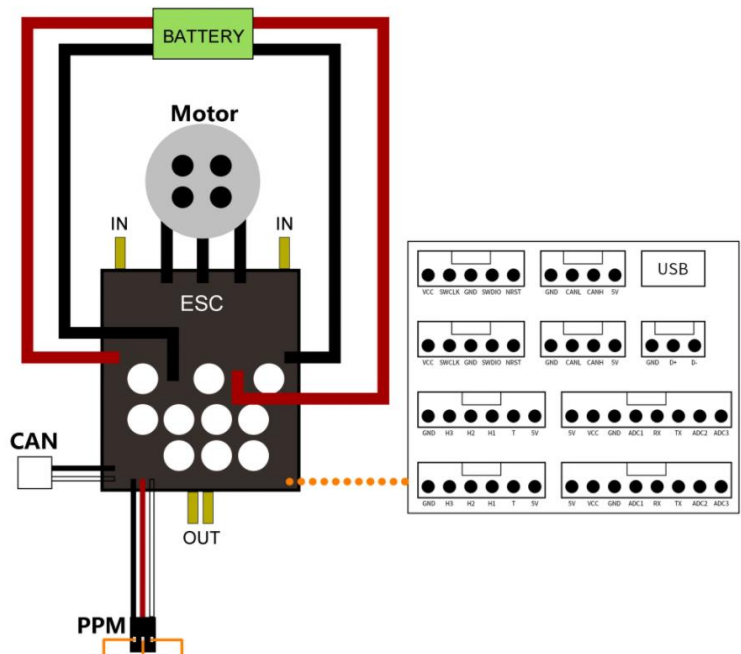


Figure 21: Flipsky ESC breakout diagram copied from [38]

This VESC (Figure 21) is rated as per [38]:

1. Input DC voltage between 8V-60V.
2. Continuous output current of 200A with bursts up to 800A.

This ESC can deliver twice as much output current as a Trampa ESC, thereby increasing power available to foil.

5.1.4 Grayhill 3D70 Display



Figure 22: Grayhill 3D70 display sample image copied from [39].

The 3D70 [39] is a 7-inch backlit Linux-based display with dual CAN-bus inputs, 800MHz clock, 512MB RAM, and 4GigaByte storage. It supports a maximum brightness of 1000nits, boot-up time of less than 3 seconds, and has an operating voltage range of 8V-32V. Applications for this display can be developed in Qt, and comes with libraries to support QML integration with modern versions of Qt.

Additionally, this display has four digital and two analog inputs as well as four digital outputs. Both CAN-bus ports on the device are independent and can be configured to run at different baud rates. Lastly, this display is IP67 ingress protection rated, making it a perfect fit for a personal watercraft.

5.2 Software Used

5.2.1 VESC Tool

VESC Tool is an open-source software from the vesc-project [40]. It allows configuration of VESC controllers, CAN property configuration, updating firmware, and generation of real-time data for testing and analysis while the controllers are operational.

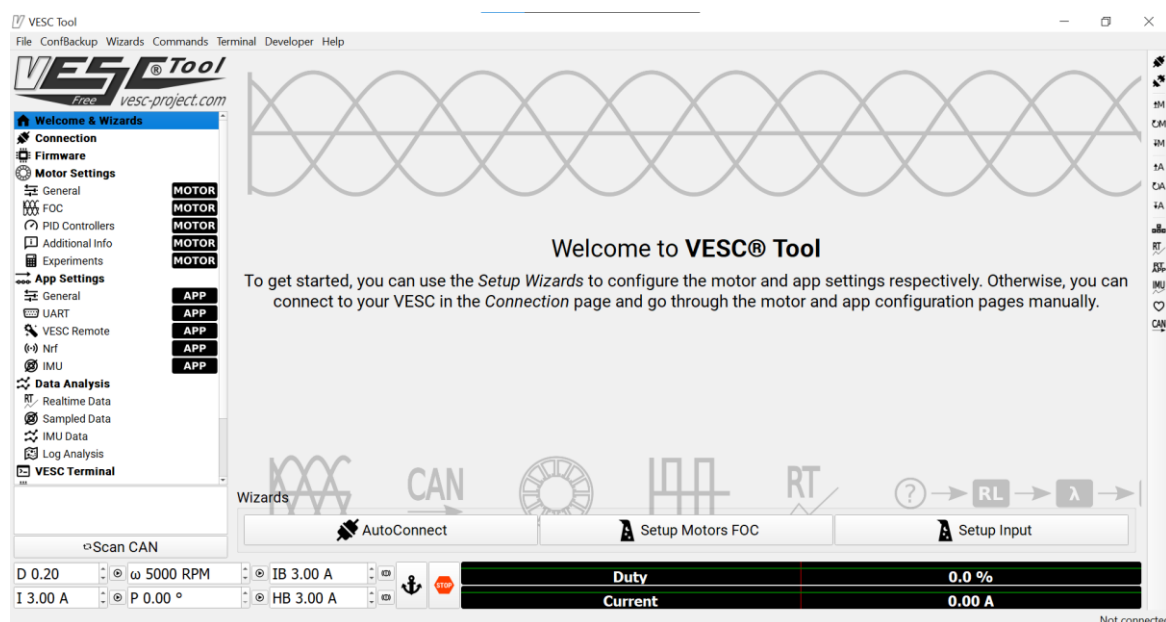


Figure 23: VESC Tool

This tool allows auto-detection of current configuration of connected VESC controllers, saving configurations to be reused later, and help wizards at each phase to allow better understanding of the tool. The VESC tool is community-driven so all resources available online are mainly the user forum and on GitHub.

5.2.2 Qt Creator

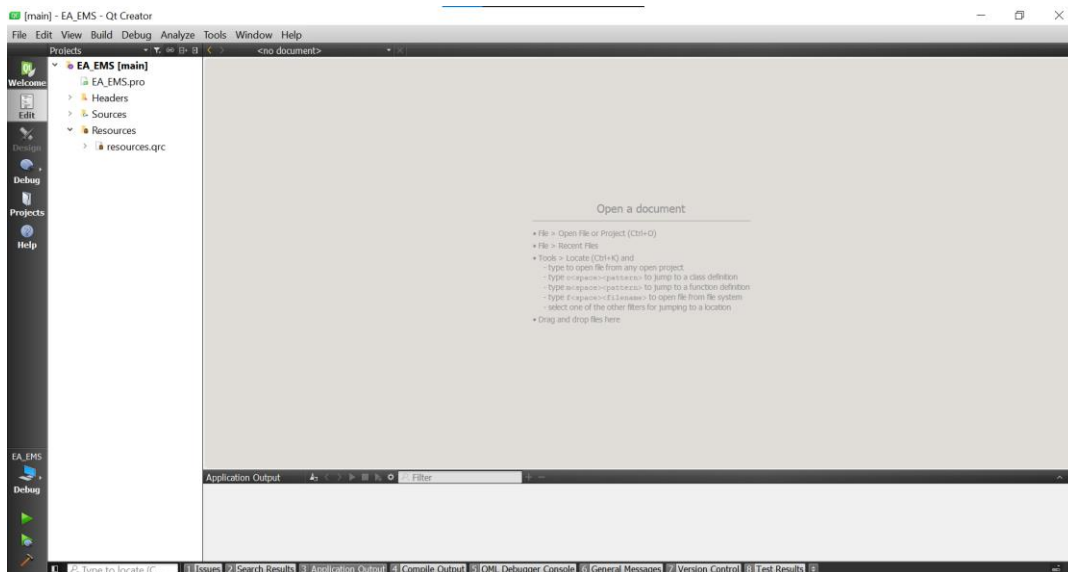


Figure 24: Qt Creator Project Window

Qt Creator is a “cross-platform integrated development environment (IDE)” [41] that can run on Windows, macOS, and Linux operating systems. Qt Creator supports active development of applications that run on mobile platforms, desktops, as well as embedded systems. It comes bundled with a code editor that supports C++, QML, Python, and JavaScript. Moreover, Qt Creator also provides a User-Interface (UI) Designer within its IDE for developers to design interactive GUIs on supported devices.

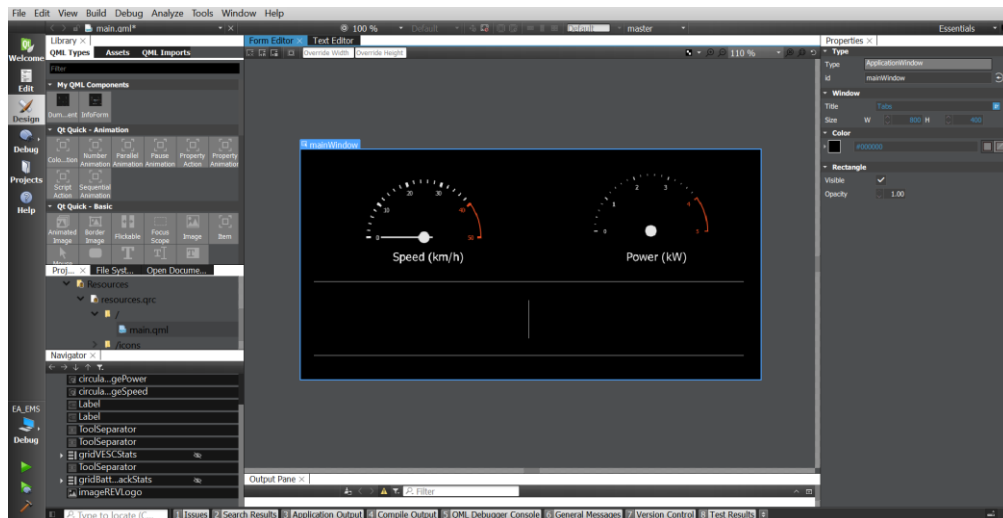


Figure 25: Qt Creator UI Designer

QML widgets can be dragged-and-dropped into UI design with the functionality to add behaviour to these elements using the accompanying text editor. Widget element appearance and performance can also be modified using the text editor.

6. Methodology

The objective of this project is to achieve automated height control and banking of the ski, while also integrating suitable motor controllers, appropriate GUI elements, and CAN-architecture to support the automated tasks. Algorithms used in the pursuit of automated control are discussed in this section using relevant Unified Modelling Language (UML) diagrams.

6.1 Control Overview

Figure 26 demonstrates overall control flow of the hydrofoil ski. Once the ski is powered on, Kalman predictive error estimation filters are initialised. This occurs for fifteen seconds during which inputs and outputs are disabled – the APM2.7 will not respond to any of the input signals. Alongside filter initialisation, serial port peripherals are also configured. Depth sensor and Global Positioning System (GPS) modules are connected to the APM2.7.

Once all initialisation is complete, ski enters a permanent loop in which all inputs are read by the APM2.7, output gains are adjusted, and outputs are actuated. This repeats consistently until the ski is powered off.

This block is independent of the hardware used – the same principles can be implemented on any controller/processor.

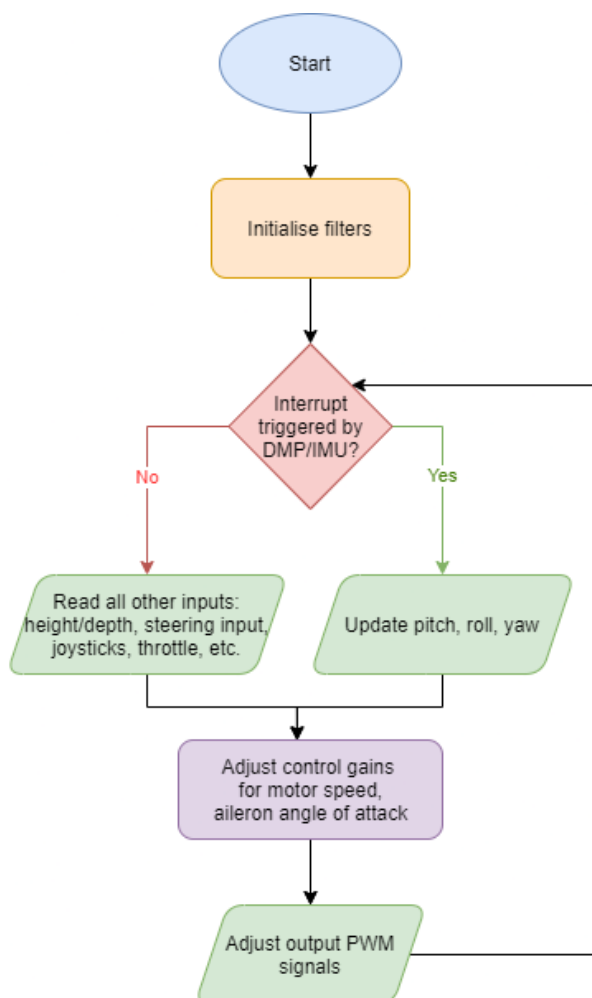


Figure 26: Overall control UML

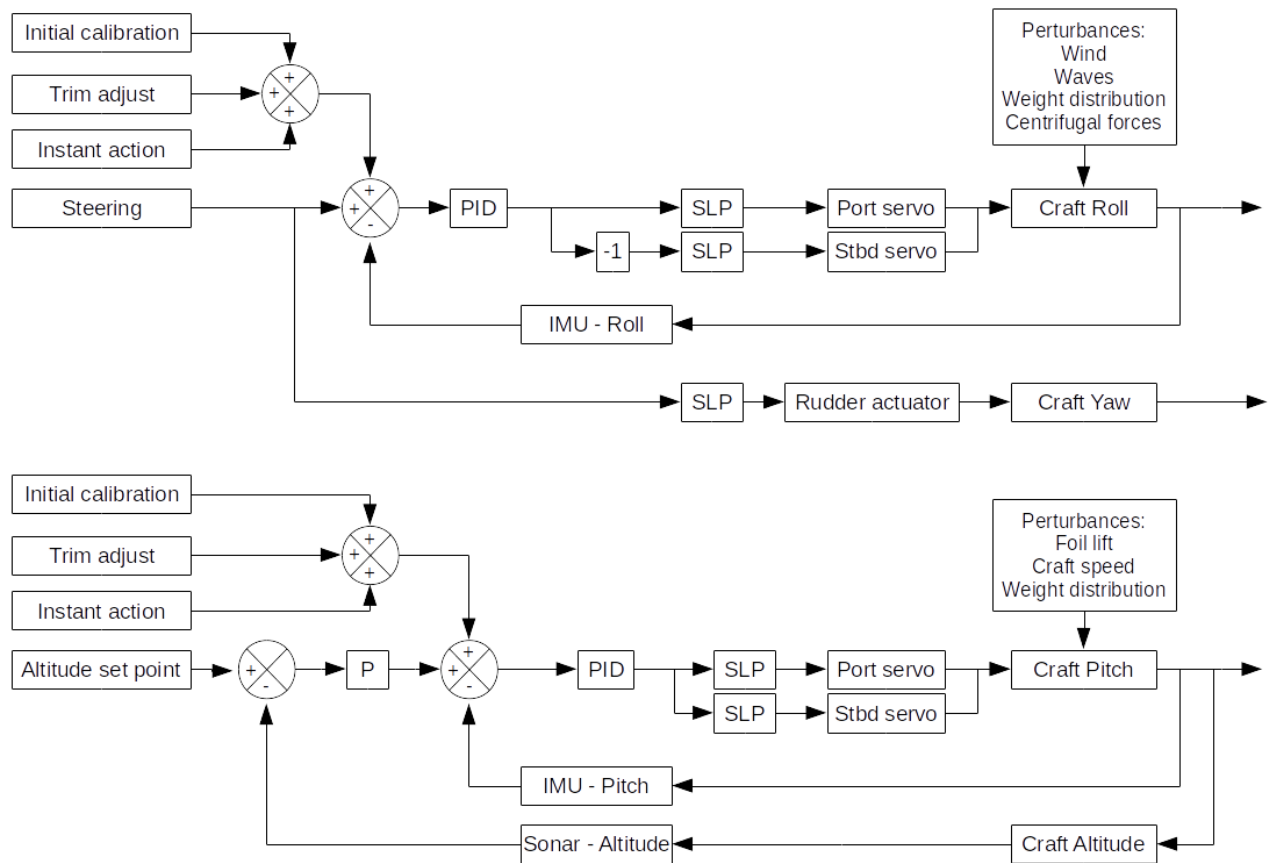


Figure 27: Control Loop Simplified Diagram

Figure 27 demonstrates the PID control loops implemented in the APM2.7. The diagrams are split into height (altitude) and banking (yaw) controls for ease of understanding. The actual implementation consists of mixing of different signals by assigning experimentally derived weights to them and effecting the actuation on the same ailerons for both height and banking.

Calibration parameters, gains, and weights given to different inputs and feedback signals are tuned experimentally to obtain the best fit for the ski. Water trials are conducted with different set of parameters that are altered based on an experienced ski rider's feedback.

Initial calibration occurs when the ski is switched on with the ski in central position. Parameters such as steering zero mark are obtained here once filters are initialised.

6.2 Height Control

Input from the height sensor is polled over serial communication at a baud rate of 9600. Target height to be achieved by ski above water surface is currently set at 30cm. A difference (error) between desired height and current height is calculated and servo PWM adjusted to compensate. PID control is applied on the servo motors. As actual height nears desired height, difference is closer to zero and hence, PWM applied to the servos is also lesser.

When actual height is less than desired height, ailerons are lowered to increase lift on the foils and raise the ski. When actual height is more than desired height, ailerons are lifted to decrease lift on the foils and lower the ski. The UML indicating this loop is in Figure 28.

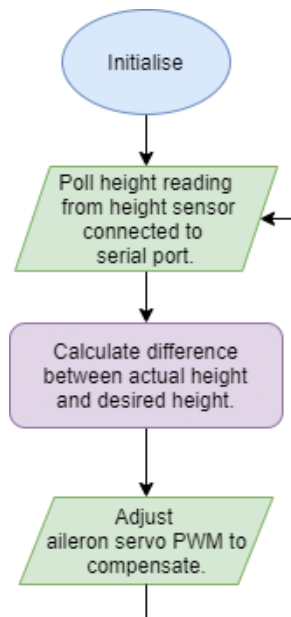


Figure 28: Height control UML

6.3 Banking Control

Banking, or more broadly turning, of the craft is achieved by moving both ailerons in opposite directions respective to each other. When foiling, ailerons alone are sufficient to produce banking. However, when the craft is on water surface and has not started foiling, ailerons are ineffective, and banking is to be achieved either through differential control of motors or by implementing a rudder like those used in traditional watercrafts. Such a situation arises since ailerons are more effective when bulk of the craft is in air and not crashing against waves. Waves require tremendous force to overcome as well as produce unnecessary yaw movement.

In Figure 29, adjusting servo PWM controls aileron angles while adjusting motor PWM individually for motors causes differential drive.

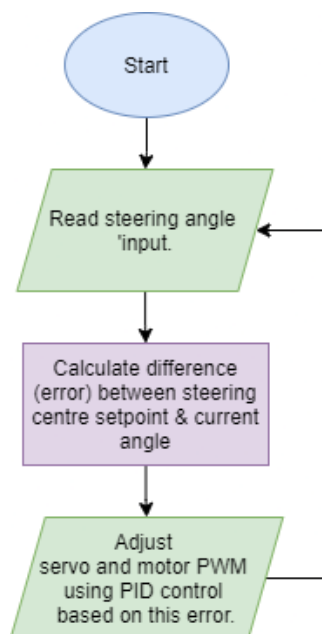


Figure 29: Banking control overview

6.3.1 Motor differential drive

Differential drive is tested to turn the craft when it is on the surface of water with a rigid rear mechanism in the absence of a rudder.

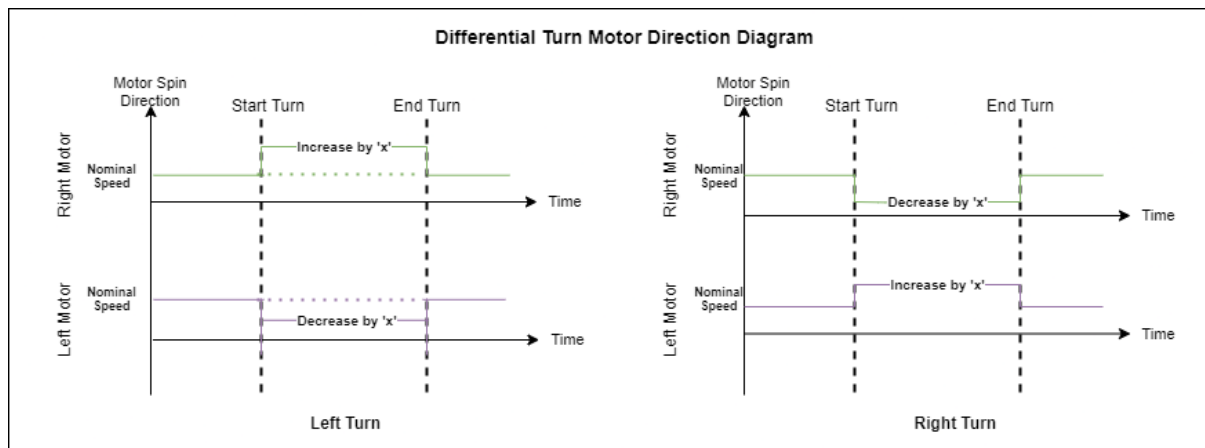


Figure 30: Differential turn motor movement direction

Difference in speeds of motors is used to make the ski turn when it is on water surface and has not begun foiling yet. Principles explained in section 4.1.6 are implemented here to achieve turns. If starboard motor is faster than port motor, ski should turn left whereas if port motor is faster than starboard motor, ski should turn right. Both motors are increased/decreased proportionally around their nominal speeds. A timing waveform of surface turning is given in Figure 30. Both motors are kept spinning in the same direction to avoid motor cogging. Their relative speeds are varied, making one run between 33% and 50% faster than the other.

This method, however, failed to produce any turn actuation. The hydrodynamic profile of the foils is potentially too rigid and span of the hydrofoils too narrow to produce the sufficient torque needed to turn the craft. Further hydrodynamic modelling is required to be performed by mechanical engineers. A rudder should be added in future scope to actuate the turn on water surface.

6.3.2 Foiling turn (pure aileron control)

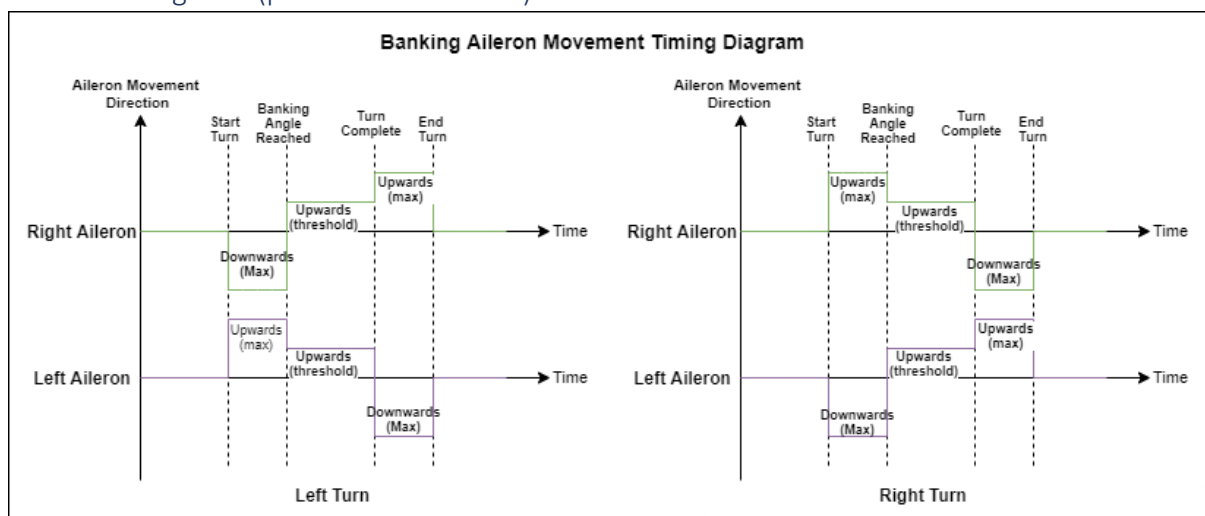


Figure 31: Aileron movement direction when banking

When foiling, both motors are kept at the same speed, making the responsibility of banking entirely that of the ailerons. This is done to maintain foiling speed to produce an effective banking angle to generate turn. Craft roll is generated depending on which of the ailerons is raised. Since when one aileron is raised the other is lowered, controlling their angle of movement controls the banking produced as depicted in Figure 31.

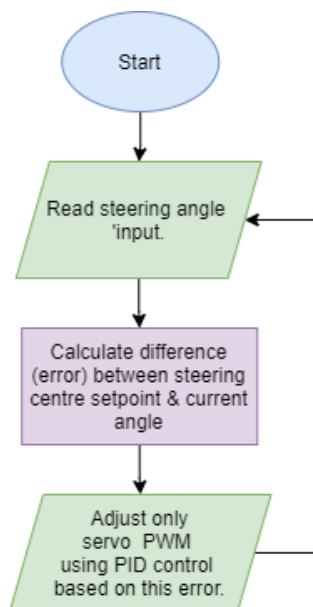


Figure 32: Turning UML when ski is foiling.

6.4 VESC Integration

VESC Tool was used to configure motor control parameters. Trampa VESC produced abrupt motor cog and had issues with supplying sufficient current for lift. Flipsky ESCs eliminated motor cog altogether and produced better performance. Overall resistance, inductance, flux linkage, and gain parameters configured for both motors are as per Table 6-1.

Table 6-1: Motor parameters

Motor Parameters:	Port	Starboard
Resistance (mΩ)	20.1	24.2
Inductance (μH)	5.36	5.22
Flux Linkage (mWb)	4.779	4.887
Current gain (Kp)	0.0054	0.0052
Current gain (Ki)	20.05	24.22
Observer gain	43.79	41.87

MOSFET temperatures, input and output currents, and PWM duty cycle are transmitted over CAN line and logged in the Grayhill display.

Appendix D contains information on configuring CAN packet transmission in VESCs. CAN bus architecture designed connects motor controllers to the CAN bus going to the display. This bus is polled by the display every 10ms and logged depending on what the packet contains. All this transmission happens at a baud rate of 250Mbps. VESC Packets are decoded as per Appendix C.

6.5 GUI Design

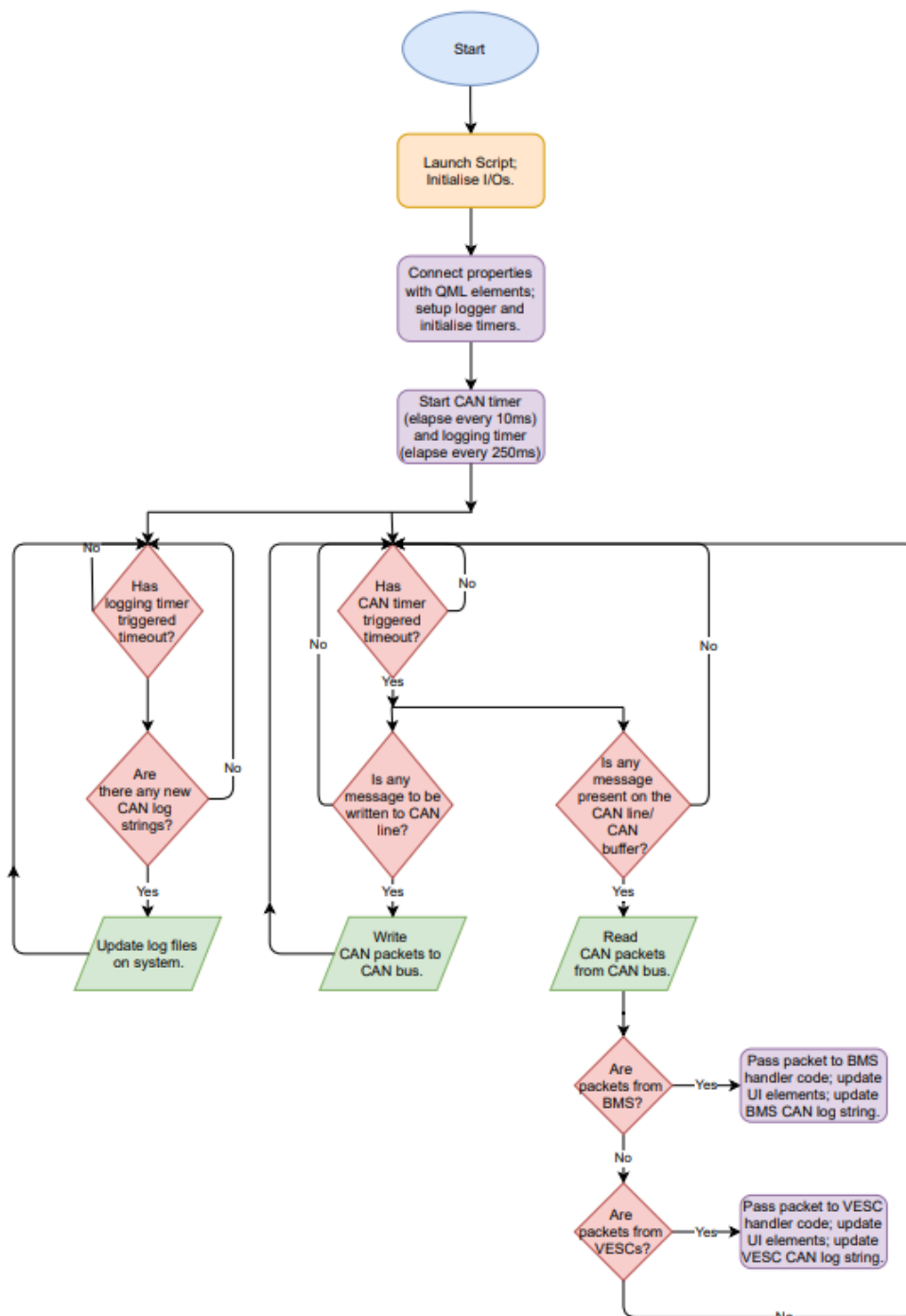


Figure 33: Display application UML

Methodology followed for the display’s application is formed of the following simple steps:

1. Automatically load appropriate script on screen boot-up.
2. Connect QML widgets with main backend code.
3. Look for any packets on CAN line. If found, sort them and handle according to packet received.
4. Log frames as required and repeat.

7. Results and Discussions

7.1 Height Control



Figure 34: Stable height 'foiling'

As demonstrated by Figure 34, stable foiling at a set height is achieved. The rider can adjust trim on the ailerons to either increase or decrease their height if desired but is not critical to achieve foiling. The control system effectively lifts and maintains craft above water surface. Implemented design makes use of a single ultrasonic sensor connected towards the middle of the craft for a more balanced pitch control. Slight turbulence is experienced in the event of rough waters with coarse waves.

7.2 Banking Control



Figure 35: 15° banking of hydrofoil ski

Craft banking is performed at a banking angle of 15° . This results in a large turning radius, irrespective of speed of travel. With an increase in roll when turning, craft goes close to the water surface but maintains foiling. This is demonstrated in Figure 35 which shows banking of the foil in real world. This control is achieved through just the steering handle – no joystick input from the rider is necessary.

7.3 CAN integration & GUI

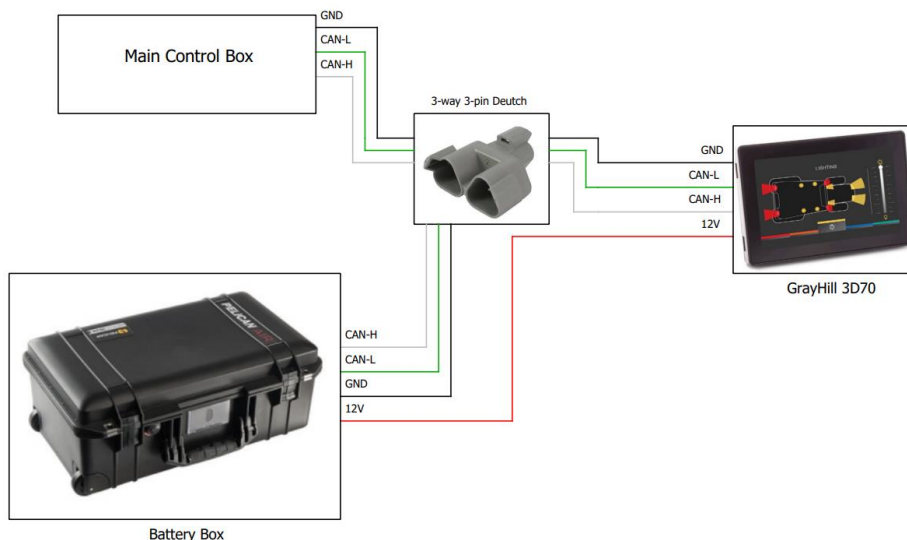


Figure 36: Hydrofoil Ski CAN Bus Schematic

Integrating a single CAN architecture across all electronics within the ski enabled displaying as well as logging of different kind of data transmitted over CAN line on the display. Figure 36 depicts the use of a 3-way 3-pin Y-shaped Deutsch connector to bridge the line between ski’s three main elements – the battery box, the display, and the main control box.

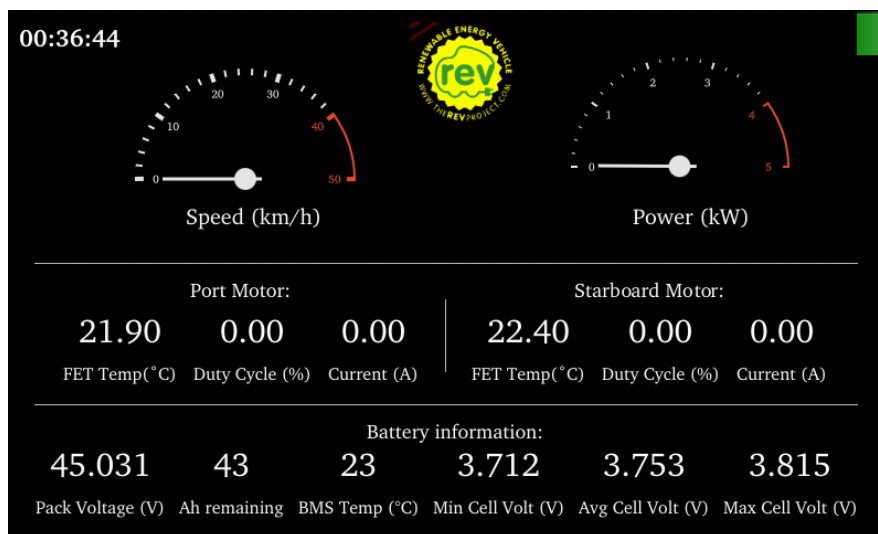


Figure 37: Final implemented GUI on Grayhill 3D70

New GUI includes easy to identify elements such as gauges for speed and power, battery status indicator, and readings from each VESC as well as the battery box individually. Brightness of the display is set to maximum to facilitate sunlight readability. By using elements like those found on instrument clusters, absorption of information from the display is more natural for the rider. All GUI design is done in C++ and QML using cross-platform compilers, allowing the same code base to be modified and compiled by any member of the development team.

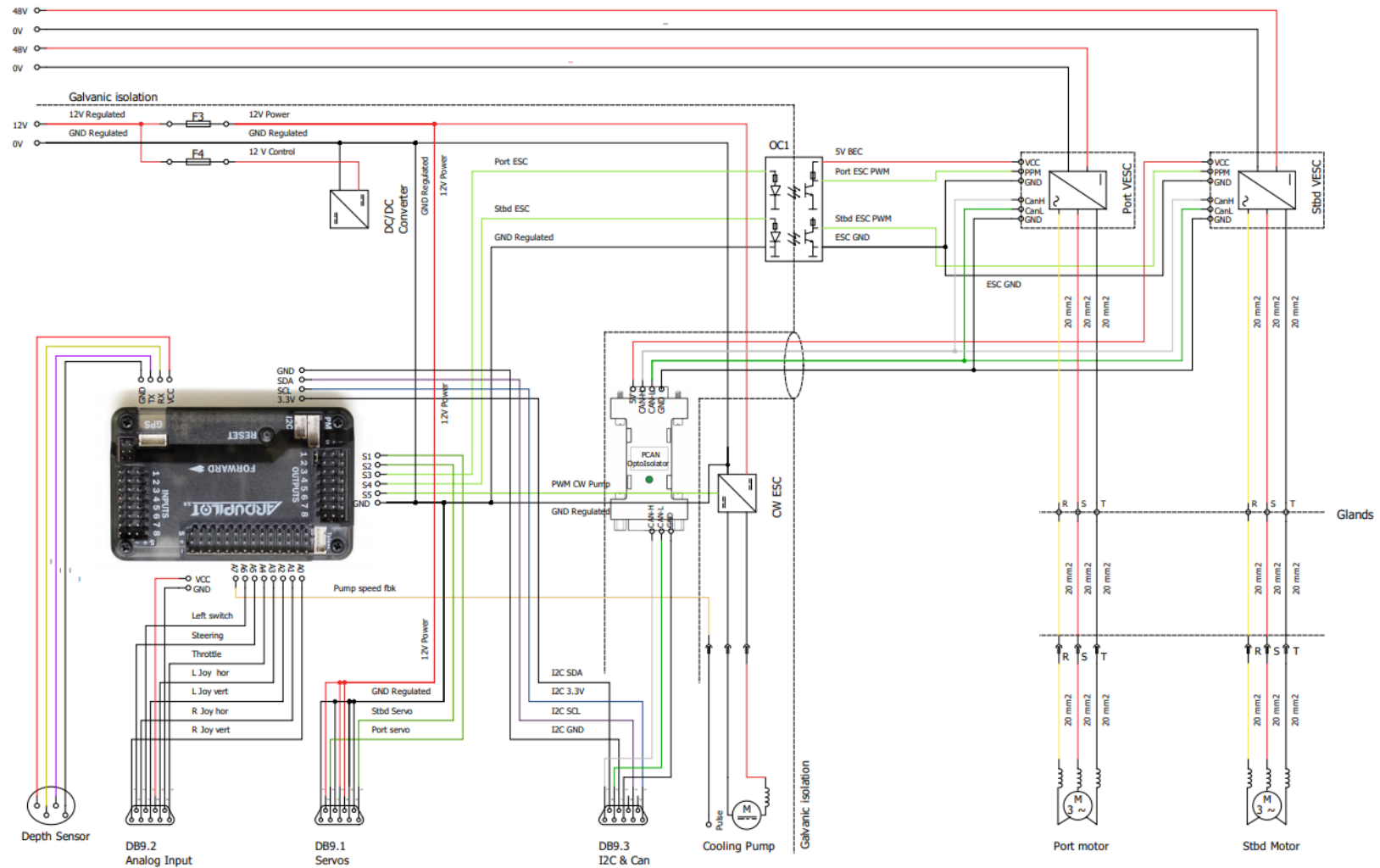


Figure 38: Control Box Wiring Schematic

7.4 Wiring & Control Box Organisation

Figure 38 represents the schematic wiring diagram of all the different components within the ski that enabled interfacing of different sensors and actuation of outputs resulting in foiling, or ‘flying state’, of the ski. Thickness of all wires used is in accordance with the currents each of them are required to pass through. All wiring in the main control box is done physically – no printed circuit board (PCB) has been designed over the course of this work.

7.5 Performance

With motor controllers throttles to run at no more than 2kW each, maximum foiling speeds of 19.8kmph are achieved as shown by the speed logged in Figure 40. With an improved controller having an integrated CAN port, higher speeds can be targeted. Installed battery pack is:

$$50V \times 240A = 12kWh$$

Keeping 2kWh in reserve, the pack can supply a peak of 10kWh. Achieving faster speeds is therefore possible but not in the scope of this thesis.

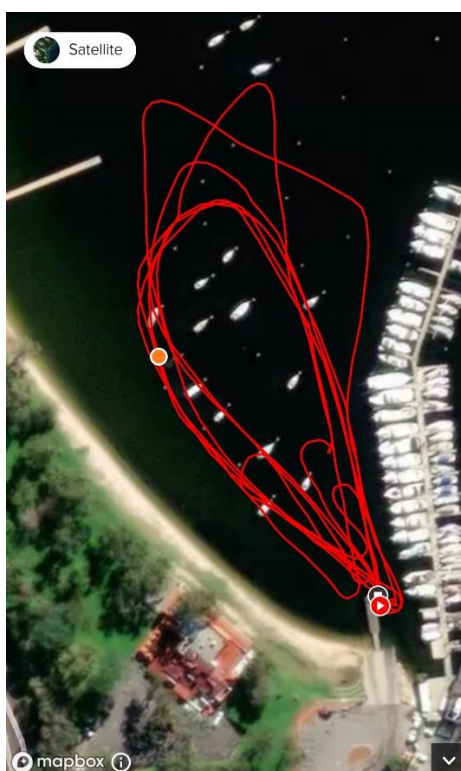


Figure 39: Test riding route



Figure 40: Speed plot for a test run

8. Conclusion and Future Scope

A fully functional hydrofoil electric ski is successfully designed and implemented in the course of this work. PID control has emerged most viable for a control system of this complexity. For the existing foil designs, differential drive did not yield any yaw control on the foil, sparking considerations of designs with a rudder mechanism.

Further improvements can be made to enhance the performance, range, and stability of the craft. A few categories in which future work can be taken up are as follows. Better waterproofing is required especially with the display that logs data – in the most recent water trial the ski capsized causing permanent water damage to the Grayhill 3D70, resulting in a complete loss of all logged data.

8.1 Controller

There are several improvements that can be made to the hydrofoil ski's control system, beginning with the IMU and processors used. As per [42], options of more accurate IMU readers exist that can provide better readings for increased stability compared to the default IMU that comes with the APM2.7.

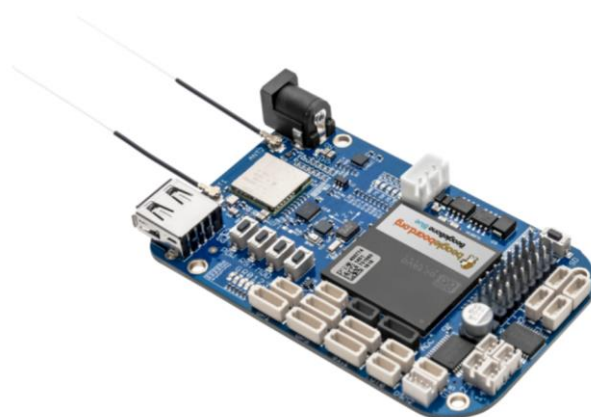


Figure 41: BeagleBone Blue, copied from [43].

Additionally, a controller that can communicate over CAN will be advantageous to transmit relevant data to the display and move to sensors that provide output over CAN, increasing the robustness of the communication architecture present within the ski. The BeagleBone Blue [43], with multiple integrated ports and programming options, is an ideal candidate to replace the APM2.7.

8.2 Hardware modules & Telemetry

Banking angle must be adjusted according to the speed of the craft much like turning of motorcycles for better stability. To achieve this, a GPS module needs to be integrated. This can be done by either interfacing a GPS module with the BeagleBone Blue or with the display directly that can then be displayed to the rider as well as transmitted to the controller.

Using an android tablet in place of the Grayhill 3D70 can also be explored since some tablets [44], are waterproof and have GPS, Bluetooth, and logging capabilities built in. Development of display UI could be done using Qt and the UI developed for Grayhill – the codebase merely needs to be tweaked and compiled for the tablet instead.



Figure 42: Samsung waterproof tablet with GPS, Bluetooth Figure 42

Inclusion of a servo-motor or linear-actuator based rudder can be explored to control banking depending on craft's altitude and speed. Waterproofing is a mandatory requirement for these products.

Wireless telemetry system is a necessity for remote parameter tuning as well as data logging, both features required for prototype development that the APM2.7 lacks.

8.3 Printed Circuit Board (PCB) Design

A PCB must be designed once all components have been finalised to minimise weak wiring links in the network and to provide an integrated control solution occupying minimum space within the ski if the prototype is to be commercialised. The PCB designed must accommodate all sensors used, except for those mounted at the steering handle for user input, close to the control board to minimise noises and increase energy efficiency.

9. References

- [1] The Personal Watercraft Industry Association, "The History, Evolution, and Profile of Personal Watercraft," 2006.
- [2] International Energy Agency, "Global EV Outlook 2020," 2020.
- [3] Australian Renewable Energy Agency, "Electric Vehicles," Australian Government, 24 August 2020. [Online]. Available: <https://arena.gov.au/renewable-energy/electric-vehicles/>. [Accessed 6 September 2020].
- [4] UWA REV Project, "REV Electric Jetski," The University of Western Australia, [Online]. Available: <https://therevproject.com/vehicles/jetski.php>. [Accessed 6 September 2020].
- [5] UWA REV Project, "REV Hydrofoil WaveFlyer," The University of Western Australia, [Online]. Available: <https://therevproject.com/vehicles/hydrofoil.php>. [Accessed 6 September 2020].
- [6] T. Rosado, "Reports on how things work - Hydrofoils," MIT, [Online]. Available: <https://web.mit.edu/2.972/www/reports/hydrofoil/hydrofoil.html>. [Accessed 15 September 2020].
- [7] S. Liu, H. Niu, L. Zhang and C. Xu, "The Longitudinal Attitude Control of the Fully-Submerged Hydrofoil Vessel Based on the Disturbance Observer," *37th Chinese Control Conference (CCC)*, pp. 397-401, 2018.
- [8] R. Bencatel, S. Keerthivarman, I. Kolmanovsk and A. Girard, "Full State Feedback Foiling Control for America's Cup Catamarans," *IEEE Transactions on Control Systems Technology*.
- [9] A. & Y. M. Muratoglu, "Performance Analysis of Hydrokinetic Turbine Blade Sections," *Advances in Renewable Energy*, vol. 2, pp. 1-10, 2015.
- [10] Hydrofoil Research Project for Office of Naval Research, Navy Department, Washington, D.C, "Hydrofoil Handbook," Gibbs and Cox, INC., New York 6, N.Y., 1954.
- [11] W. Weist, "Development of an ultrasonic ranging device for hydrofoil height control," *Ocean 73 - IEEE International Conference on Engineering in the Ocean Environment*, pp. 438-444, 1973.
- [12] D. R. Lopez, "Ailerons," National Aeronautics and Space Administration, 01 November 2018. [Online]. Available: <https://www.grc.nasa.gov/www/k-12/airplane/alr.html#:~:text=Ailerons%20are%20small%20hinged%20sections,deflected%20downward%2C%20and%20vice%20versa.&text=The%20ailerons%20are%20used%20to,wing%20tip%20to%20move%20down..> [Accessed 05 April 2021].

- [13] J. W. Tallman, "HOW IT WORKS: AILERONS," Aircraft Owners and Pilots Association (AOPA), 1 September 2019. [Online]. Available: <https://www.aopa.org/news-and-media/all-news/2019/september/flight-training-magazine/how-it-works-aileron>. [Accessed 9 March 2021].
- [14] L. Krishna, "EI-FOIL HYDROFOIL PROFILE ANALYSIS AND REAR MECHANISM DESIGN," The University of Western Australia, 2020.
- [15] T. Bräunl, *Embedded Robotics - Mobile Robot Design and Application with Embedded Systems*, Springer.
- [16] S.-l. Yang, W. Zi, L.-x. Ma, H.-q. Zhang and Z.-l. Yang, "Optimizing-computation of Controlling Parameters of Intelligent Propulsion System of a Hydrofoil Sliding Craft Propelled by Adjustable-pitch Screw," *2009 Fifth International Joint Conference on INC, IMS and IDC*, pp. 1815-1818, 2009.
- [17] T. Kinoshita and Y. Sudo, "Overview and current state of a new single-handed hydrofoil sailing catamaran," *Oceans '04 MTS/IEEE Techno-Ocean '04 (IEEE Cat. No.04CH37600)*, vol. 2, pp. 1010-1013, 2004.
- [18] B. Porter and A. Khaki-Sedigh, "Design of digital set-point tracking PID controllers for hydrofoils," *International Conference on Control - CONTROL 88, Oxford, UK*, pp. 660-665, 1988.
- [19] A. C. Kermode, *Mechanics of Flight*, 11th Edition, Pearson Education, 2006.
- [20] R. Mathew and S. S. Hiremath, "Trajectory tracking and control of differential drive robot for predefined regular geometrical path," *Global Colloquium in Recent Advancement and Effectual Researchers in Engineering, Science and technology*, pp. 1273-1280, 2016.
- [21] A. Draou, "Electronic differential speed control for two in-wheels motors drive vehicle," *4th International Conference on Power Engineering, Energy and Electrical Drives*, pp. 764-769, 2013.
- [22] National Instruments, "Controller Area Network (CAN) Overview," National Instruments (NI), 1 September 2020. [Online]. Available: <https://www.ni.com/en-in/innovations/white-papers/06/controller-area-network--can--overview.html>. [Accessed 6 September 2020].
- [23] S. Corrigan, "Introduction to the Controller Area Network (CAN)," Texas Instruments, 2016.
- [24] H. Othman, Y. Aji, F. Fakhreddin and A. Al-Ali, "Controller Area Networks: Evolution and Applications," in *IEEE 2nd International Conference on Information & Communication Technologies*, Damascus, 2006.
- [25] G. MacDonald, "Do you need a Lithium Battery Management System?," *Lithium Battery Systems*, [Online]. Available:

- <https://www.lithiumbatterysystems.com.au/lithium-battery-management-system-required/>. [Accessed 6 September 2020].
- [26] Battery University, “BU-908: Battery Management System (BMS),” Battery University, [Online]. Available: https://batteryuniversity.com/learn/article/how_to_monitor_a_battery. [Accessed 6 September 2020].
- [27] The Qt Company, “Qt Features,” [Online]. Available: <https://www.qt.io/product/features>. [Accessed 12 February 2021].
- [28] The Qt Company, “About Qt,” [Online]. Available: https://wiki.qt.io/About_Qt. [Accessed 2 December 2020].
- [29] The Qt Company, “Qt Quick,” [Online]. Available: https://wiki.qt.io/Qt_Quick. [Accessed 2 December 2020].
- [30] ArduPilot, “ArduPilot Mega,” ArduPilot, [Online]. Available: ardupilot.co.uk.
- [31] SAMSUNG SDI, *SPECIFICATION OF PRODUCT - Lithium-ion rechargeable cell for power tools Model name: INR18650-30Q*, SAMSUNG SDI Energy Business Division.
- [32] 18650battery.com, “Samsung 30Q 18650 3000mAh 15A Battery,” [Online]. Available: <https://www.18650battery.com/Samsung-18650-p/samsung-30q.htm>. [Accessed 6 September 2020].
- [33] ZEVA, “8-16 Cell Integrated Battery Management System,” ZEVA, [Online]. Available: <https://www.zeva.com.au/index.php?product=135>. [Accessed 6 September 2020].
- [34] ZEVA, *BMS16v2 User Manual*.
- [35] ZEVA, *BMS16v2 CAN Protocol Manual*, ZEVA.
- [36] TRAMPA, “VESC 6 MKIV In CNC T6 Silicone Sealed Aluminium Box with Genuine XT90 Connectors - Vedder Electronic Speed Controller TRAMPA Special,” TRAMPA, [Online]. Available: <https://trampaboards.com/vesc-6-mkiv-in-cnc-t6-silicone-sealed-aluminium-box-with-genuine-xt90-connectors--vedder-electronic-speed-controller-trampa-special-p-27536.html>. [Accessed 6 September 2020].
- [37] B. Vedder, *Vedder ESC for DC and BLDC Motors (Datasheet)*, TRAMPA.
- [38] Flipsky, “High Current FSESC 200A 60V base on VESC6,” Flipsky, [Online]. Available: <https://flipsky.net/collections/electronic-products/products/high-current-fsesc-200a-60v-base-on-vesc6>. [Accessed 6 April 2021].
- [39] Grayhill, Inc., *Versatile CAN-Based Display*.
- [40] B. Vedder, “VESC Tool,” vesc-project, [Online]. Available: https://vesc-project.com/vesc_tool. [Accessed 7 September 2020].

- [41] The Qt Company, “Qt Creator - A cross-platform IDE for Application Development,” [Online]. Available: <https://www.qt.io/product/development-tools>. [Accessed 6 April 2021].
- [42] L. Xu, “Low-Cost Sensor Based Orientation Detection System for,” The University of Western Australia, 2020.
- [43] BeagleBoard.org, “BeagleBone Blue,” BeagleBoard.org, [Online]. Available: <https://beagleboard.org/blue>. [Accessed 20 March 2021].
- [44] Samsung Australia, “Samsung Galaxy Tab Active 3,” Samsung, [Online]. Available: <https://www.samsung.com/au/business/tablets/galaxy-tab-active3-t575/smt575nzkaxsa/>. [Accessed 16 June 2021].
- [45] Arduino, “Arduino Software,” Arduino, [Online]. Available: <https://www.arduino.cc/en/main/software>. [Accessed 7 September 2020].
- [46] B. Vedder, “Benjamin's Robotics,” 7 January 2015. [Online]. Available: <http://vedder.se/2015/01/vesc-open-source-esc/>. [Accessed 28 March 2021].
- [47] J. Valdez and J. Becker, “Understanding the I2C Bus,” Texas Instruments, 2015.
- [48] Y. Fujiwara, “Self-Synchronizing Pulse Position Modulation With Error Tolerance,” *IEEE Transactions on Information Theory*, vol. 59, no. 9, pp. 5352-5362, 2013.

Appendix A: Extended CAN Frame

1. SOF: Start-of-Frame bit marking start of a message.
2. SRR: Substitute remote request (Remote Transmission Request in Standard CAN). This is dominant when information is required from a different node.
3. IDE₂: Identifier extension indicates when more bits are to follow, and extended addressing is being used.
4. Identifier: establishes priority of message being transmitted. A higher priority is assigned to a lower binary value.
5. r1, r0: reserved unused bits. Can be used for future expansion.
6. DLC: 4-bit data length code that indicates number of bytes of data being transmitted.
7. Data: main data being transmitted. Can be up to 8 bytes.
8. CRC: 16-bit cyclic redundancy check containing checksum for error detection.
9. ACK: acknowledgement sent back indicating if accurate error-free data has been received.
10. EOF: 7-bit pack indicating End-of-Frame.
11. IFS: 70bit interframe space which contains the time required for controller to properly buffer a received frame.

Appendix B: BMS CAN Protocol

1. Broadcast Status: BMS broadcasts this information packet at 4Hz.

	Bit 7	Bit 6	Bit 5	Bit 4	Bit 3	Bit 2	Bit 1	Bit 0
Byte 0	Error code					Status code		
Byte 1	Battery amp-hours remaining, 0.1Ah resolution, high byte							
Byte 2	Battery amp-hours remaining, 0.1Ah resolution, low byte							
Byte 3	Battery voltage, 0.1V resolution, high byte							
Byte 4	Battery voltage, 0.1V resolution, low byte							
Byte 5	Reserved							
Byte 6	Reserved							
Byte 7	Temperature (°C+40)							

Table 0-1: BMS Status Transmitted Packet obtained from [35]

2. Cell Voltages: all cell voltages are transmitted by BMS in a similar format with different numbering depending on the packets. ID xx1 contains the first four (1-4) cell voltages, ID xx2, contains the next four (5-8), and so on.

	Bit 7	Bit 6	Bit 5	Bit 4	Bit 3	Bit 2	Bit 1	Bit 0
Byte 1	Voltage 1, high byte							
Byte 2	Voltage 1, low byte							
Byte 3	Voltage 2, high byte							
Byte 4	Voltage 2, low byte							
Byte 5	Voltage 3, high byte							
Byte 6	Voltage 3, low byte							
Byte 7	Voltage 4, high byte							
Byte 8	Voltage 4, low byte							

Table 0-2: Cell Voltage packets from BMS16 copied from [34]

Appendix C: VESC6 CAN Protocol

Status Message ID	Packet Status	Buffer	Information Value
1	9	Byte 0	RPM 4 bytes [31:0]
		Byte 1	
		Byte 2	
		Byte 3	
		Byte 4	Total current in all units (times 10)
		Byte 5	Latest duty Cycle (time 1000)
		Byte 6	
		Byte 7	
2	14	Byte 0	Total Amp Hours consumed by unit (times 10,000)
		Byte 1	
		Byte 2	
		Byte 3	
		Byte 4	Total regenerative amp hours put back in battery (times 10,000)
		Byte 5	
		Byte 6	
		Byte 7	
3	15	Byte 0	Total Watt Hours consumed by unit (times 10,000)
		Byte 1	
		Byte 2	
		Byte 3	
		Byte 4	Total regenerative Watt hours put back in battery (times 10,000)
		Byte 5	
		Byte 6	
		Byte 7	
4	16	Byte 0	MOSFET Temperature (times 10)
		Byte 1	Motor Temperature (times 10)
		Byte 2	
		Byte 3	Total input current (times 10) in amps
		Byte 4	
		Byte 5	
		Byte 6	Current PID position
Byte 7			
5	27	Byte 0	Tachometer readings (probably rpm)
		Byte 1	
		Byte 2	
		Byte 3	
		Byte 4	Input voltage (times 10) in amps
		Byte 5	
		Byte 6	Reserved
Byte 7			

Table 0-1: CAN status packets transmitted by VESC-6

Appendix D: VESC Tool ESC CAN Configuration

CAN configuration of motor controllers

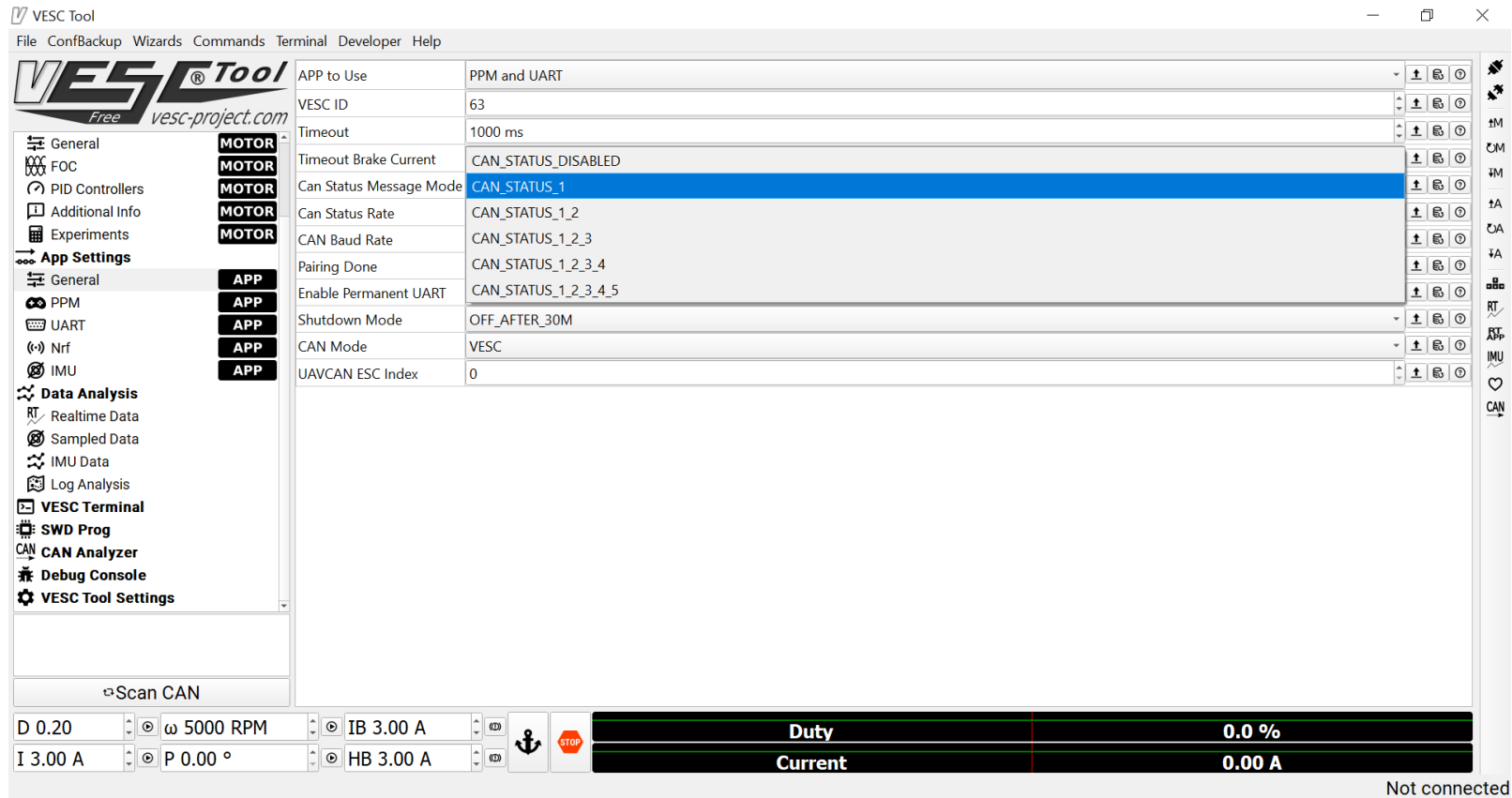


Figure 43: CAN settings on VESC Tool